Dielectric magnetic microparticles as photomagnonic cavities: Enhancing the modulation of near-infrared light by spin waves

Evangelos Almpanis*

Institute of Nanoscience and Nanotechnology, NCSR "Demokritos," Patriarchou Gregoriou and Neapoleos St., Agia Paraskevi, GR-153 10 Athens, Greece

(Received 31 January 2018; revised manuscript received 20 April 2018; published 3 May 2018)

The coupling between spin waves and optical Mie resonances inside a dielectric magnetic spherical particle, which acts simultaneously as a photonic and magnonic (photomagnonic) cavity, is investigated by means of numerical calculations accurate to arbitrary order in the magnetooptical coupling coefficient. Isolated dielectric magnetic particles with diameters of just a few microns support high-Q optical Mie resonances at near-infrared frequencies and localized spin waves, providing an ultrasmall and compact platform in the emerging field of *cavity optomagnonics*. Our results predict the occurrence of strong interaction effects, beyond the linear-response approximation, which lead to enhanced modulation of near-infrared light by spin waves through multimagnon absorption and emission mechanisms.

DOI: 10.1103/PhysRevB.97.184406

I. INTRODUCTION

Controlling the interaction of light with magnetization dynamics provides impressive opportunities in the development of contemporary, fast and energy-efficient magnetic recording and signal-processing technologies [1,2]. Photons have already been considered as a forthcoming alternative to electrons through the development of photonic circuits [3–5] while magnons (the quanta of spin waves) are very promising candidates as information agents for low-energy-cost computing and data storage [6–8], and their precise and efficient control becomes feasible with the use of the so called *magnonic crystals* [7,8] and *magnonic metamaterials* [9,10]. Obviously, combing the desirable properties of both photons and magnons and controlling their mutual interaction by the utilization of hybrid photonic-magnonic nanostructures could be the key for the development of novel devices.

The fact that microwave photons interact efficiently with magnons inside appropriately designed cavities, has paved the way to the emergence of *cavity spintronics* [11] field. In the general concept, a magnetic resonator is placed inside a microwave cavity resulting in a strong coupling between the magnons supported by the resonator and the cavity photons [12–24]. This can lead to a plethora of intriguing phenomena such as strong coupling in the quantum limit [12,13], high and ultra-high cooperativity interactions [20,21] and magnetostriction [19]. At microwave frequencies, the formation of cavity-magnon-polaritons [15,16] inside millimeter-sized dielectric magnetic particles becomes also possible. Generally, a magnetic insulating material that attracts most of the interest and is commonly used in such applications is yttrium iron garnet (YIG). YIG combines optical transparency with gyromagnetic behavior at microwave frequencies [16,22–24] and sustains long-lifetime magnonic excitations, which is crucial for spintronics applications. In all of the above-mentioned microwave-cavity setups there is a direct conversion between microwave photons and magnons, due to the matching of their frequencies. However, as it will be discussed later, this is not the case when we refer to the interaction of visible/near-infrared photons with magnons, where coupling originates from the change in the dielectric permittivity tensor of the material induced by the dynamic evolution of the magnetization and the aforementioned strong-coupling effects do not take place.

Scattering of visible/near-infrared light by magnons, has long been the subject of Raman and Brillouin light scattering (BLS) spectroscopy [25–39] for the detection of spin-wave excitations in materials while, also, Bragg diffraction by magnetostatic waves finds applications in optical signal-processing [40–42]. More recently, BLS spectroscopy acquired renewed interest in the detection and/or probing of spin waves down to the micro/nano-scale [37]. In this context, there has been a significant very recent activity on BLS studies in the so-called *optomagnonic* or *photomagnonic* cavities [43–54] that act simultaneously as cavities for visible/near-infrared photons and magnons, increasing their corresponding lifetimes, and thus enhancing their inherently weak interaction. A ubiquitous concept is the utilization of spherical magneto-optical (MO) whispering gallery mode resonators, where enhanced inelastic scattering of light by spin waves takes place [44–46]. The above-mentioned photomagnonic coupling is based on the gyroelectric properties of a magnetized garnet material, such as YIG. More recently, planar photomagnonic nanocavities for triggering multimagnon absorption and emission processes by a photon have also been proposed [51]. Nevertheless, a thorough study of such interaction processes in particle-type photomagnonic micro/nano-cavities is still lacking.

In the present work we examine the case of such a spherical photomagnonic cavity, with diameter of a few microns, which manifests multimagnon scattering processes with near-infrared light. A homogeneous sphere of a dielectric magnetic material that sustains simultaneously localized spin waves and optical Mie resonances is considered. Due to the huge frequency mismatch between the frequencies of the magnons ($1 \sim 100$ GHz) and photons ($200 \sim 400$ THz) involved, a

*ealmpanis@gmail.com

quasistatic approximation is applied for a precise calculation of the dynamical photomagnonic interaction.

II. THEORY

A. Mie resonances of a dielectric magnetic sphere

At first, we assume a harmonic, monochromatic, plane electromagnetic (EM) wave, of angular frequency ω and wave vector $\mathbf{q}_0$, propagating in air. The associated electric field component has the general form $\mathbf{E}_0(\mathbf{r},t) = Re[\hat{\mathbf{e}}E_0 \exp[i(\mathbf{q}_0 \cdot \mathbf{r} - \omega t)]] = Re[\mathbf{E}_0(\mathbf{r}) \exp(-i\omega t)]$, where for $\hat{\mathbf{e}} = \hat{\boldsymbol{\theta}}_1$ or $\hat{\mathbf{e}} = \hat{\boldsymbol{\theta}}_2$ the wave is termed as p- or s-linear polarized, with $\hat{\boldsymbol{\theta}}_1$ and $\hat{\boldsymbol{\theta}}_2$ being the polar and azimuthal unit vectors, respectively, which are perpendicular to $\mathbf{q}_0$. The above-mentioned plane wave can be expanded into regular vector spherical waves, about a given origin of coordinates, as follows

$$\mathbf{E}_0(\mathbf{r}) = \sum_{\ell m} \left[a^0_{1\ell m} j_\ell(qr)\mathbf{X}_{\ell m}(\hat{\mathbf{r}}) + \frac{i}{q_0} a^0_{2\ell m} \nabla \times j_\ell(qr)\mathbf{X}_{\ell m}(\hat{\mathbf{r}}) \right], \tag{1}$$

where j_ℓ are spherical Bessel functions and $\mathbf{X}_{\ell m}$ vector spherical harmonics, which are defined in terms of the usual (scalar) spherical harmonics, $Y_{\ell m}$, through the equation $\sqrt{\ell(\ell+1)}\mathbf{X}_{\ell m}(\hat{\mathbf{r}}) = -i\mathbf{r} \times \nabla Y_{\ell m}(\hat{\mathbf{r}})$, for $\ell \geqslant 1$, while $\mathbf{X}_{00}(\hat{\mathbf{r}}) = 0$. The spherical-wave amplitudes, $a^0_{P\ell m}$, $P = 1$ (magnetic polarization mode), 2 (electric polarization mode), $\ell = 1,2,\ldots$ and $m = -\ell, -\ell+1, \ldots \ell$, can be written in the form [55]

$$a^0_{P\ell m} = \mathbf{A}^0_{P\ell m}(\hat{\mathbf{q}}_0) \cdot \hat{\mathbf{e}} E_0, \tag{2}$$

with

$$\begin{aligned} \mathbf{A}^0_{1\ell m}(\hat{\mathbf{q}}_0) = \frac{4\pi i^\ell (-1)^{m+1}}{\sqrt{\ell(\ell+1)}} \{ & \left[\alpha^m_\ell \cos\theta e^{i\phi} Y_{\ell-m-1}(\hat{\mathbf{q}}_0) \right. \\ & + m \sin\theta Y_{\ell-m}(\hat{\mathbf{q}}_0) + \alpha^{-m}_\ell \cos\theta e^{-i\phi} Y_{\ell-m+1}(\hat{\mathbf{q}}_0) \left. \right] \hat{\boldsymbol{\theta}}_1 \\ & + i \left[\alpha^m_\ell e^{i\phi} Y_{\ell-m-1}(\hat{\mathbf{q}}_0) - \alpha^{-m}_\ell e^{-i\phi} Y_{\ell-m+1}(\hat{\mathbf{q}}_0) \right] \hat{\boldsymbol{\theta}}_2 \} \end{aligned} \tag{3}$$

and

$$\begin{aligned} \mathbf{A}^0_{2\ell m}(\hat{\mathbf{q}}_0) = \frac{4\pi i^\ell (-1)^{m+1}}{\sqrt{\ell(\ell+1)}} \{ & i \left[\alpha^m_\ell e^{i\phi} Y_{\ell-m-1}(\hat{\mathbf{q}}_0) \right. \\ & \left. - \alpha^{-m}_\ell e^{-i\phi} Y_{\ell-m+1}(\hat{\mathbf{q}}_0) \right] \hat{\boldsymbol{\theta}}_1 \\ & - \left[\alpha^m_\ell \cos\theta e^{i\phi} Y_{\ell-m-1}(\hat{\mathbf{q}}_0) + m \sin\theta Y_{\ell-m}(\hat{\mathbf{q}}_0) \right. \\ & \left. + \alpha^{-m}_\ell \cos\theta e^{-i\phi} Y_{\ell-m+1}(\hat{\mathbf{q}}_0) \right] \hat{\boldsymbol{\theta}}_2 \} , \end{aligned} \tag{4}$$

where $\alpha^m_\ell = \frac{1}{2}[(\ell-m)(\ell+m+1)]^{1/2}$; θ and ϕ denote the angular variables of $\mathbf{q}_0$ in the chosen system of spherical coordinates.

Let us now assume a homogeneous magnetically saturated sphere located at the origin of the coordinate system. In general, the optical response of static magnetic materials, in the visible and near-infrared parts of the spectrum, is described by a relative magnetic permeability $\mu = 1$ and a relative electric permittivity tensor [56], $\bar{\bar{\epsilon}}(\mathbf{M})$, which depends on the magnetization $\mathbf{M} = (M_x, M_y, M_z)$. To first order in the magnetization, the relative electric permittivity tensor is given by [51]

$$\bar{\bar{\epsilon}}(\mathbf{M}) = \begin{pmatrix} \epsilon & if\frac{M_z}{M_s} & -if\frac{M_y}{M_s} \\ -if\frac{M_z}{M_s} & \epsilon & if\frac{M_x}{M_s} \\ if\frac{M_y}{M_s} & -if\frac{M_x}{M_s} & \epsilon \end{pmatrix} \tag{5}$$

with M_s being the saturation magnetization and f the dimensionless Faraday coefficient [57]. If the material is magnetically saturated along the z axis, Eq. (5) takes the simple form

$$\bar{\bar{\epsilon}} = \begin{pmatrix} \epsilon & if & 0 \\ -if & \epsilon & 0 \\ 0 & 0 & \epsilon \end{pmatrix}. \tag{6}$$

When a plane EM wave is incident on the spherical particle, it is scattered by it and the scattered field can also be expressed into vector spherical waves, as follows

$$\begin{aligned} \mathbf{E}_{\rm sc}(\mathbf{r}) = \sum_{\ell m} \Big[& a^+_{1\ell m} h^+_\ell(q_0 r)\mathbf{X}_{\ell m}(\hat{\mathbf{r}}) \\ & + \frac{i}{q_0} a^+_{2\ell m} \nabla \times h^+_\ell(q_0 r)\mathbf{X}_{\ell m}(\hat{\mathbf{r}}) \Big], \end{aligned} \tag{7}$$

where h^+_ℓ are spherical Hankel functions of the first kind. The amplitudes of the scattered spherical waves, a^+_{Plm}, are linearly related to their counterparts of the incident field, a^0_{Plm}, through the so-called scattering T matrix, which can be evaluated by requiring the boundary conditions at the surface of the sphere to be satisfied by the EM field. For an unmagnetized homogeneous sphere, the T matrix is diagonal in $P\ell m$ and independent of m because of the spherical symmetry of the scatterer. However, this is not the case for a magnetized (gyrotropic) sphere where its dielectric permittivity tensor is given by Eq. (6). Explicit forms of the T-matrix elements for such a sphere can be found elsewhere [58] and several T-matrix studies of single gyrotropic scatterers or collections of such have been reported [59–61]. We just note here that, for a sphere magnetized along the z direction, the T matrix has a block diagonal form: $T_{P\ell m;P'\ell'm'} = T^{(m)}_{P\ell;P'\ell'}\delta_{mm'}$, where $T^{(m)}_{P\ell;P'\ell'}$ vanish identically if the magnetic/electric multipoles corresponding to $P\ell$ and $P'\ell'$ do not have the same parity, even or odd. This means that the T matrix in a given subspace is further reduced into two submatrices with different symmetry, also termed as *gerade* (even) and *ungerade* (odd). Given these considerations, a group-theory [62] methodology can be applied to elucidate the symmetry properties of the Mie resonances of such a magnetized sphere, saturated along the z axis. The symmetry transformations of a gyrotropic sphere form the $C_{\infty h}$ point group, as described in Table I. Each *gerade* and *ungerade* submatrix corresponds to a one-dimensional

TABLE I. Character table for the $C_{\infty h}$ point group.

$C_{\infty h}$	E	C_ϕ	I	IC_ϕ
A_g	1	1	1	1
A_u	1	1	−1	−1
E_{mg}	1	$e^{im\phi}$	1	$e^{im\phi}$
E_{mu}	1	$e^{im\phi}$	−1	$-e^{im\phi}$

TABLE II. Projection of a plane EM wave propagating at an angle θ with respect to the z axis, of s or p polarization, on the basis of irreducible representations of $C_{\infty h}$.

Angle of incidence	Polarization	$C_{\infty h}$
$\theta = 0,\pi$	s or p	$E_{\pm 1g}, E_{\pm 1u}$
$\theta \neq 0,\pi/2,\pi$	s	$A_u, A_g, E_{\pm 1g}, E_{\pm 1u}, E_{\pm 2g}, E_{\pm 2u}, \ldots$
	p	$A_u, A_g, E_{\pm 1g}, E_{\pm 1u}, E_{\pm 2g}, E_{\pm 2u}, \ldots$
$\theta = \pi/2$	s	$A_u, E_{\pm 1g}, E_{\pm 2u}, E_{\pm 3g}, E_{\pm 4u}, \ldots$
	p	$A_g, E_{\pm 1u}, E_{\pm 2g},, E_{\pm 3u}, E_{\pm 4g}, \ldots$

irreducible representation A_g, E_{mg} or A_u, E_{mu}, respectively. Representations A_g, A_u refer to $m = 0$, while E_{mg}, E_{mu} to $m = \pm 1, \pm 2, \ldots$. In order to excite a specific optical resonance, the symmetry of the incident field should be compatible to that of the resonant mode, as listed in Table II and detailed below. Similarly to the case of a nonspherical axisymmetric scatterer [63], for incidence along the axis of magnetization ($\theta = 0,\pi$) it results from Eqs. (3) and (4) that $|\mathbf{A}^0_{P\ell m} \cdot \hat{\mathbf{e}}|^2 = (2\ell + 1)\pi\delta_{|m|1}$ and thus s- or p-polarized waves can only excite states of $E_{\pm 1g}$ or $E_{\pm 1u}$ symmetry. For $\theta = \pi/2$, an s-polarized wave excites only modes with $P + \ell + m$: even while a p-polarized wave excites only modes with $P + \ell + m$: odd, because only in these cases we have $|\mathbf{A}^0_{P\ell m} \cdot \hat{\mathbf{e}}|^2 \neq 0$. On the contrary, for $\theta \neq 0,\pi/2,\pi$ both polarizations are able to excite all, i.e. A_u, A_g, E_{mg}, E_{mu}, modes, although to a different degree, depending on the specific mode profile.

We note that, if the magnetization direction of the magnetized sphere does not coincide with the z axis of the laboratory frame, an appropriate transformation of the T matrix is needed. In general, if α,β,γ are the Euler angles [64] transforming an arbitrarily chosen coordinate system in which the magnetization is oriented along the z axis, the T matrix is given by

$$T_{P\ell m;P'\ell' m'} = \sum_{m''} D^{(\ell)}_{mm''}(\alpha,\beta,\gamma) T^{(m'')}_{P\ell;P'\ell'} D^{(\ell')}_{m''m'}(-\gamma,-\beta,-\alpha), \tag{8}$$

where $D^{(\ell)}_{mm'}(\alpha,\beta,\gamma)$ are the appropriate transformation matrices associated with the ℓ irreducible representation of the $O(3)$ group [62]. However, in such a case the T matrix no longer has a block-diagonal form. For the sake of completeness, we note here that a similar Mie-scattering formalism has also been developed for gyromagnetic scatterers characterized by an appropriate magnetic permeability tensor [16,65,66] which is relevant to microwave frequencies. However, in the visible and near-infrared part of the spectrum that we consider here, the magnetized scatterer has only gyroelectric response.

B. Inelastic light scattering by the homogeneous precession spin wave

So far, we considered statically magnetized particles, where the magnetization is oriented along a given axis. The excitation of a spin wave in such a particle corresponds to a dynamic magnetization field, which induces a spatiotemporal perturbation in the electric permittivity tensor. In the present work we shall be concerned with the uniform precession spin mode [42] in a magnetic dielectric sphere, and we will be restricted to small spin-wave amplitudes. Since this, so-called Kittel, mode is equivalent to a homogeneous periodic variation, with period Ω, of the magnetization vector, when the precession is about the z axis, the corresponding magnetization field has the form [51]

$$\begin{aligned}\mathbf{M}(t)/M_s &= m_x(t)\hat{\mathbf{x}} + m_y(t)\hat{\mathbf{y}} + \hat{\mathbf{z}} \\ &= \eta\cos(\Omega t)\hat{\mathbf{x}} + \eta\sin(\Omega t)\hat{\mathbf{y}} + \hat{\mathbf{z}},\end{aligned} \tag{9}$$

where η is the amplitude of the spin wave. This field profile, at any particular time snapshot, describes a sphere homogeneously magnetized along an axis which is different from z. The new axis, at a given time t, can be expressed in terms of the Euler angles α, β, and γ, where we have $\alpha = \Omega t$, $\sin\beta = \eta$, and $\gamma = 0$. The total electric permittivity tensor in the presence of the spin wave is written as $\bar{\bar{\epsilon}} + \delta\bar{\bar{\epsilon}}(z,t)$, with $\bar{\bar{\epsilon}}$ given by Eq. (6) and

$$\begin{aligned}\delta\bar{\bar{\epsilon}}(t) &= \begin{pmatrix} 0 & 0 & -if\eta\sin(\Omega t) \\ 0 & 0 & if\eta\cos(\Omega t) \\ if\eta\sin(\Omega t) & -if\eta\cos(\Omega t) & 0 \end{pmatrix} \\ &\equiv \frac{1}{2}[e^{-i\Omega t}\delta\bar{\bar{\epsilon}} + e^{i\Omega t}\delta\bar{\bar{\epsilon}}^{\dagger}],\end{aligned} \tag{10}$$

with

$$\delta\bar{\bar{\epsilon}} = f\eta\begin{pmatrix} 0 & 0 & 1 \\ 0 & 0 & i \\ -1 & -i & 0 \end{pmatrix}, \tag{11}$$

where we restricted ourselves to leading order, i.e., to first order in the spin-wave amplitude and neglected the small Cotton-Mouton contributions.

Since the periodic variation of the magnetization is relatively slow we can introduce time-dependent coefficients $a^+_{P\ell m}(t)$ for the scattered field [67] that result from a time-dependent T matrix, and assume them to be constant over a period of the EM wave (quasistatic approximation). In this regime, the dynamic evolution of the problem is described at a sequence of snapshots of the magnetization precession, by the corresponding T matrix given by Eq. (8) if we substitute the appropriate Euler angles at each time snapshot. Hence, the scattering cross section is calculated as

$$\sigma_{sc}(t) = \frac{1}{q_0^2|\mathbf{E}_0|^2}\sum_{P\ell m}|a^+_{P\ell m}(t)|^2. \tag{12}$$

Since the time variation of $\sigma_{sc}(t)$ is periodic, with constant frequency Ω, it can be expanded into a Fourier series

$$\sigma_{sc}(t) = \sigma_{sc}(t + 2\pi/\Omega) = \sum_{n=0,\pm 1,\ldots}\bar{\sigma}^{(n)}_{sc}e^{-in\Omega t}. \tag{13}$$

Consequently, for a monochromatic incident optical wave of angular frequency ω, the scattered field consists of an infinite number of beams with angular frequencies $\omega + n\Omega$, $n = 0,\pm 1,\pm 2,\ldots$, where $\bar{\sigma}^{(n)}_{sc}$ corresponds to the elastic ($n = 0$) and inelastic ($n \neq 0$) scattering intensities, respectively. When strong inelastic scattering processes take place, there will be significant probabilities for absorption and/or emission of multiple magnons by a photon. On the other hand, when the photomagnonic interaction is weak, the corresponding Fourier

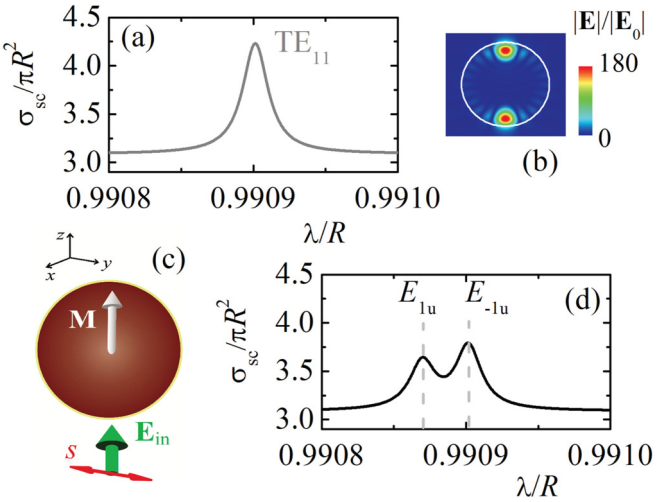

FIG. 1. (a) Normalized scattering cross section spectrum of an unmagnetized Bi:YIG sphere, with radius R, in the proximity of the TE_{11} Mie resonance, for linearly polarized incident light. (b) Corresponding electric field profile on a plane parallel to the polarization plane, cutting through the center of the sphere, at the TE_{11} resonance frequency. (c) Schematic view of a Bi:YIG sphere with radius R magnetized along the z axis, where light impinges along the magnetization axis. (d) Normalized scattering cross section spectrum for linearly polarized incident light on the magnetically saturated Bi:YIG sphere shown in (c). The two nondegenerate modes that correspond to $m = \pm 1$ are marked with vertical dashed lines.

spectrum is essentially dominated by the first-order terms which correspond to one-magnon exchange processes. We note that we are working in the linear spin-wave regime neglecting magnon-magnon interactions since such effects have not been observed or considered in garnet particles [43–46,48,50,52–54].

III. RESULTS AND DISCUSSION

A. Optical response of a statically magnetized garnet sphere

In the present work we consider a dielectric magnetic sphere of radius R, in air, which will serve as a photomagnonic cavity. Dielectric magnetic particles of rare-earth iron garnets with sizes ranging from millimeters to nanometers can be fabricated in the laboratory by various techniques [43,68–70]. Our calculations were performed for a bismuth-substituted yttrium iron garnet (Bi:YIG) spherical particle in the near-infrared part of the spectrum, where the relative magnetic permeability is equal to unity and the values of dielectric permittivity tensor of Eq. (6) are $\epsilon = 5.5$ and $f = -0.01$ [71]. Our results are presented in scaled wavelength units λ/R, where the radius R of the sphere can vary roughly from 800 to 1500 nm to adjust the optical mode under consideration in the near-infrared region. Such an unmagnetized sphere ($f = 0$) supports high-Q, spectrally separated, multipole (2^{ℓ}-pole) Mie resonances of transverse magnetic ($P = 1$) and transverse electric ($P = 2$) type, which confine the field inside the particle. The optical response in the proximity of the transverse electric mode with $\ell = 11$ (TE_{11}) which is manifested as a peak in the scattering cross section, is shown in Fig. 1(a). The corresponding electric-field profile in the plane of polarization is displayed in Fig. 1(b). This particular resonance has a 23-fold degeneracy which corresponds to $2\ell + 1$ values of the m angular momentum index. In the case of such a magnetically saturated sphere, the $(2\ell + 1)$-fold degeneracy is lifted with the frequency shift depending on the strength of the MO interaction. However, for light incident along the direction of magnetization, as shown in Fig. 1(c), only 2 out of the 23 modes can be excited according to group theory, namely those with symmetry $E_{\pm 1u}$. This is clearly illustrated in Fig. 1(d), where only two resonances appear in the scattering cross-section spectrum. The lower frequency (higher λ/R) mode has the E_{-1u} symmetry since it originates from the corresponding $T^{(m=-1)}_{P\ell;P'\ell'}$ submatrix, with $P + \ell$ and $P' + \ell'$ being odd (*ungerade*). Similarly, the higher frequency (lower λ/R) mode has the E_{1u} symmetry since it originates from the corresponding $T^{(m=1)}_{P\ell;P'\ell'}$ submatrix. In the given configuration, these two modes are excited by right-circularly polarized (RCP) ($m = -1$) and left-circularly polarized (LCP) ($m = 1$) incident light, respectively. Since an incident linearly polarized light beam is a superposition of a RCP and a LCP wave, it excites both eigenmodes. The splitting of the nondegenerate modes depends on the strength of the MO interaction. By increasing the MO coupling coefficient f, the splitting between the modes becomes more pronounced. However, in this work we assume a magnetically saturated sphere, and thus the coefficient f cannot be further increased by the external magnetic field. Consequently, any further increase of the splitting could only be achieved from an increase of the mode lifetime (higher-Q) which is possible for higher multipole modes (higher-ℓ). Alternatively, an increase in the mode splitting would be possible by choosing a different magnetic material exhibiting higher refractive index and/or MO coefficient. The mode splitting will play an important role in the analysis of the photomagnonic interaction which follows and for this reason we chose a reasonable compromise between mode lifetime and particle radius, given that all other parameters originate from the material properties.

Although an incident light wave along the direction of magnetization can couple only to the modes than correspond to $m = \pm 1$, this is not the case for different angles of incidence. When light impinges at an angle, $\theta \neq 0, \pi/2, \pi$, any mode could be excited, to a certain degree, depending on the corresponding field profile, the angle of incidence and polarization of the incoming wave, as discussed in the theory section. Hence, to get a better understanding of the static MO interaction, it would be useful to study the $\theta \neq 0$ cases as well. For this purpose, in Fig. 2 we show the scattering cross section for both s and p polarizations for different values of θ angle, in the configuration shown in the inset picture. It can be clearly seen that, apart from the two major resonances of $E_{\pm 1u}$ symmetry, excited efficiently at $\theta = 0^{\circ}$, another resonance appears with significant scattering magnitude for $\theta \simeq 10^{\circ}$, which has the A_u symmetry and is efficiently excited by s-polarized incident light. Besides this, the signature of modes which correspond to higher values of $|m|$ can be identified in both spectra of Fig. 2. For the sake of convenience we have not shown all the 23 modes in Fig. 2, but roughly half of them. It is worth noting that each mode is dispersionless in frequency (it is located at the same λ/R), but there are differences between the scattering efficiency for each particular mode depending on

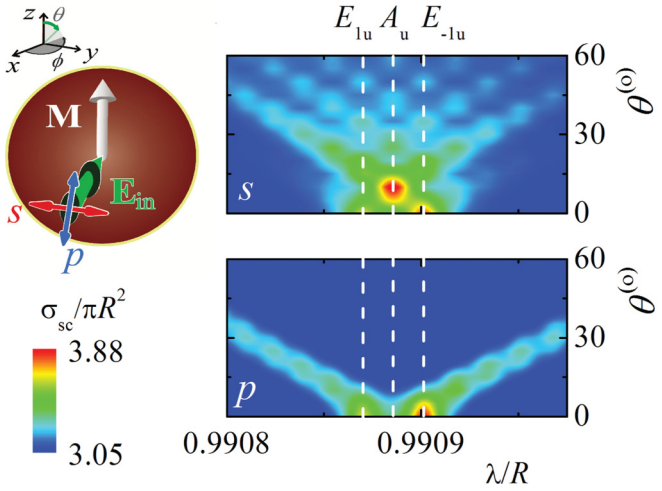

FIG. 2. Normalized scattering cross section spectrum of a magnetically saturated Bi:YIG sphere with radius R, for s (upper panel) and p (lower panel) polarized light incident at an angle θ with respect to the z axis, as shown in the margin. The central vertical line indicates the position of the mode with A_u symmetry ($m = 0$), which is excited only if $\theta \neq 0, 2\pi$, while the other two vertical lines indicate the positions of $E_{\pm 1u}$ ($m = \pm 1$) modes shown in Fig. 1(d).

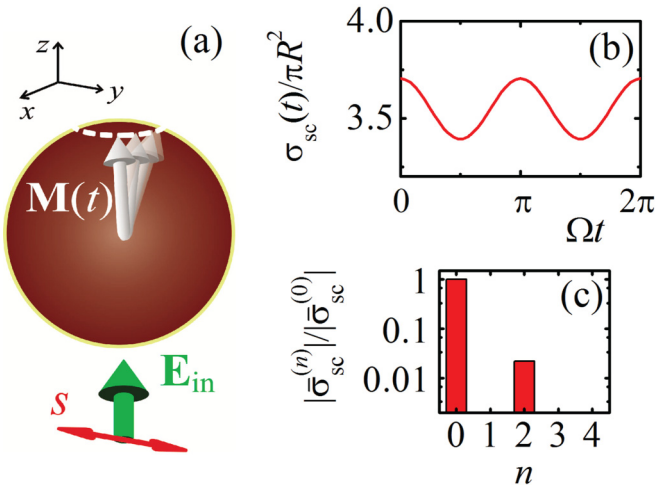

FIG. 3. (a) A schematic of the Kittel magnon mode. Magnetization undergoes a periodic uniform precession about the z axis, with angular frequency Ω. (b) Time variation of the scattering cross-section amplitude at the frequency of the A_u optical mode induced by the Kittel magnon. (c) Relative intensities of the elastically ($n = 0$) and inelastically ($n \neq 0$) scattered light beams.

the angle θ and polarization, as shown in Fig. 2. The different coupling degree between incident radiation and eigenmodes of the magnetized sphere is due to field-profile symmetry reasons, but a further investigation of each particular case is beyond the scope of the present paper. Finally, even though in the present work we shall only focus in a narrow spectral region about the central mode A_u symmetry ($m = 0$), our analysis can be directly applied to any mode.

B. Photon-magnon interaction

We now consider excitation of the uniform precession (Kittel) mode in the magnetized Bi:YIG sphere. This is the fundamental magnon mode which corresponds to a dynamic macrospin precession, as depicted in Fig. 3(a). Here we assume precession angle $\beta = 5^{\circ}$ which corresponds to a spin-wave amplitude $\eta \simeq 0.09$. The uniform precession mode is, in general, efficiently excited in small particles of magnetic dielectrics such as iron garnets [15,17–23,43–46,72,73], and the frequency of such magnons is usually several GHz. In our case, we can apply the quasistatic approximation to calculate precisely the time variation of the scattering cross section since the period of the spin wave is much longer than that of the light wave. We first assume incidence of light along the z axis ($\theta = 0$), as shown in Fig. 3(a). The dynamical magnetization precession of the Kittel mode induces a periodic variation of the permittivity tensor according to Eq. (10), resulting in a periodically time-varying $\sigma_{sc}(t)$ with frequency Ω. When inelastic photon-magnon scattering processes take place, the Fourier expansion of $\sigma_{sc}(t)$ involves also nonnegligible orders with $n > 0$ which correspond to absorption and emission probabilities of n magnons by a photon. In Fig. 3(b) we show the temporal variation of σ_{sc} for the optical resonance with wavelength $\lambda/R = 0.990885$ (symmetry A_u) at incidence of light with $\theta = 0$, within the period of the spin wave. The scattering cross section undergoes a sinusoidal variation with period π/Ω, reaching a maximum (minimum) magnitude when the magnetization component in the xy plane is perpendicular (parallel) to the polarization, which happens twice within a full precession of the magnetization vector. This is reflected on the corresponding Fourier spectrum of Fig. 3(c) where, apart from the elastic scattering component ($n = 0$), the spectrum involves only two-magnon exchange contributions ($n = 2$). Obviously, the $\sigma_{sc}(t)$ for p-polarized incident light, i.e., polarization perpendicular to that of Fig. 3, will be simply shifted by $\pi/2$, while the corresponding Fourier spectrum will be unaffected. The absence of the one-magnon processes indicates that a selection rule is imposed by the symmetry of the respective fields involved, similarly to the selection rules in planar geometries [51,74]. To first-order Born approximation, the scattering intensity of a photon by a single magnon is proportional to the overlap integral $\langle \mathbf{E}^{\rm og}(\mathbf{r})| \, \delta\bar{\bar{\epsilon}} \, |\mathbf{E}^{\rm ig}(\mathbf{r})\rangle$, where $\mathbf{E}^{\rm og}(\mathbf{r})$ and $\mathbf{E}^{\rm ig}(\mathbf{r})$ are the outgoing and ingoing electric fields inside a statically magnetized sphere along the z axis. By substituting the tensor $\delta\bar{\bar{\epsilon}}$ from Eq. (11) we obtain

$$\langle \mathbf{E}^{\rm og}(\mathbf{r})| \, \delta\bar{\bar{\epsilon}} \, |\mathbf{E}^{\rm ig}(\mathbf{r})\rangle \propto -\int_{V_{sph}} d^3r \left[E_x^{\rm ig}(\mathbf{r}) + i\,E_y^{\rm ig}(\mathbf{r})\right] E_z^{\rm og}(\mathbf{r}) + \int_{V_{sph}} d^3r \left[E_x^{\rm og}(\mathbf{r}) + i\,E_y^{\rm og}(\mathbf{r})\right] E_z^{\rm ig}(\mathbf{r}), \tag{14}$$

where V_{sph} is the volume of the spherical particle. The general form of the electric field inside a statically magnetized spherical scatterer, expanded into vector spherical harmonic waves is given in Ref. [58]. After some straightforward algebra we conclude that $[E_x^{\rm ig(og)}(\mathbf{r}) + i\,E_y^{\rm ig(og)}(\mathbf{r})]$ and $E_z^{\rm og(ig)}(\mathbf{r})$ belong to different-m irreducible representations of the $C_{\infty h}$ group. Therefore, since for light incident along the magnetization axis, m is a conserved quantity, each integral vanishes identically

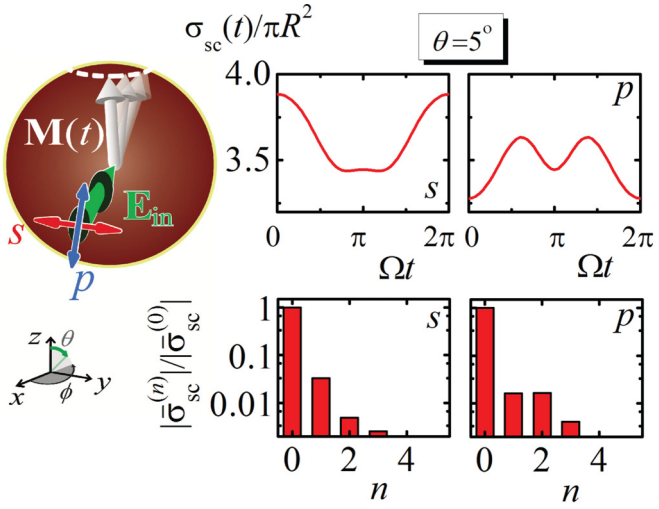

FIG. 4. Upper panels: Time variation of the normalized scattering cross section at the frequency of the A_u optical mode, induced by the Kittel magnon mode, for s (left-hand panel) and p (right-hand panel) polarized light incident at an angle $\theta = 5^\circ$, as shown in the inset graphic. Lower panels: Corresponding relative intensities of the elastically ($n = 0$) and inelastically ($n \neq 0$) scattered light beams.

leading to $\langle \mathbf{E}^{\rm og}(\mathbf{r})| \, \delta\bar{\bar{\epsilon}} \, |\mathbf{E}^{\rm ig}(\mathbf{r})\rangle = 0$. This is the reason why first-order terms are absent in the Fourier spectrum of Fig. 3(c). This is valid for any nondegenerate photonic mode of the particle, if light is incident along the z axis.

The above-mentioned selection rule though, breaks when incidence of light is not along the z axis (i.e., the plane defined by the two orthogonal polarizations is no longer parallel to the magnetization precession plane xy), and as a result we expect nonzero intensities for one-magnon exchange processes. Such dynamical optical response, associated with inelastic scattering involving $n = 1,2,3,\ldots$ magnons, is shown in Fig. 4 for linearly polarized light incident at an angle $\theta = 5^\circ$ with respect to the z axis, and an azimuthal angle $\phi = 180^\circ$, which means that the wave vector lies in the xz plane. In the left (right) hand panels of Fig. 4 we display the time variation of the scattering cross section and the corresponding Fourier components for an s-(p-)polarized incident wave, as shown in the inset graphic. Since we are working in the frame of the quasistatic approximation, it would be helpful to see some aspects of our results from the prism of the static picture discussed in the previous sections. At $\Omega t = 0$ the magnetization vector has $m_y(0) = 0$ and $m_x(0) = \eta = \sin 5^\circ$, and consequently the configuration is equivalent to light incident at an angle 10° with respect to the magnetization axis. In this case, according to Fig. 2 (at $\theta = 10^\circ$), we expect a maximum scattering magnitude for s-polarized light, and a minimum scattering efficiency for p-polarized light, as indeed can be observed in Fig. 4. Moreover, not only the two scattering cross sections start from a different value (at $t = 0$) but their whole temporal evolution is different since the symmetry of the configuration of Fig. 3 is now broken and the simple geometrical justification of a constant phase shift between the two time variations is no longer valid. On the whole, we should keep in mind that the scattering cross section in both cases undergoes abrupt changes and such a behavior can also be explained in the corpuscular picture. In particular, the Fourier components in Fig. 4 indicate that an s-polarized incident beam is inelastically scattered primarily by one-magnon- and to a lesser degree by two- and three-magnon-absorption and emission processes. On the other hand, a p-polarized light beam is scattered inelastically to almost the same extend through one- and two-magnon-absorption and emission processes, while a weaker contribution of three-magnon absorption and emission processes is also present. We additionally note here that if the m-mode splitting was not large enough, then we could not expect such abrupt changes in the scattering cross section since there would be significant contribution from other optical m modes at the same frequency resulting in a roughly constant magnitude of the scattering cross section irrespective of the angle of light incidence. As a result, strong inelastic light scattering by spin waves is expected only in cavities that induce sufficiently large mode splitting in the static MO case. This requirement can be generalized to include nonspherical particles as well. In that case, the scattering cross section of a Mie scatterer with nonspherical shape could be computed numerically at each time snapshot within one magnonic period, and thereafter substituted into Eq. (13) to obtain the corresponding Fourier intensities for the photomagnonic interaction.

IV. CONCLUSION

To conclude, we have carried out thorough calculations of the photon-magnon interaction in Bi:YIG spherical particles of only a few microns diameter. The photomagnonic coupling has been studied in the frame of the quasistatic approximation which is valid due to the significant frequency mismatch between light ($200 \sim 400$ THz) and spin waves ($1 \sim 100$ GHz). Our results show that in the presence of a spin wave, namely the homogeneous precession mode, the time-dependent optical response of the particle at a Mie resonance undergoes abrupt changes which are translated into n-magnon ($n = 1,2,3\ldots$) absorption and emission processes in the Fourier spectrum. In fact, the simultaneous concentration of both the EM field and the spin wave for a long period of time inside the particle enhances their inherently weak interaction leading to strong inelastic scattering of photons by magnons. Furthermore, this enhanced interaction can be controlled by symmetry-dependent parameters as it has been indicated from the photon-magnon overlap integral. Our work moves a step towards the miniaturization of photomagnonic cavities since until now the studies focused on dielectric magnetic particles at the millimeter scale. Hence, such ultra-small particle-type photomagnonic cavities can provide an efficient and versatile platform for tailoring the optomagnonic interaction and controlling photons with magnons.

[1] T. Satoh, R. Lida, T. Higuchi, M. Fiebig, and T. Shimura, Nat. Photon. **9**, 25 (2015).

[2] J. Walowski and M. Münzenberg, J. Appl. Phys. **120**, 140901 (2016).

[3] P. Dong, Y. K. Chen, G. H. Duan, and D. T. Neilson, Nanophotonics **3**, 215 (2014).

[4] C. P. Dietrich, A. Fiore, M. G. Thompson, M. Kamp, and S. Höfling, Laser Photon. Rev. **10**, 870 (2016).

[5] D. Thomson, A. Zilkie, J. E. Bowers, T. Komljenovic, G. T. Reed, L. Vivien, D. Marris-Morini, E. Cassan, L. Virot, J.-M. Fédéli, J.-M. Hartmann, J. H. Schmid, D.-X. Xu, F. Boeuf, P. O'Brien, G. Z. Mashanovich, and M. Nedeljkovic, J. Opt. **18**, 073003 (2016).

[6] A. V. Chumak, V. I. Vasyuchka, A. A. Serga, and B. Hillebrands, Nat. Phys. **11**, 453 (2015).

[7] M. Krawczyk and D. Grundler, J. Phys.: Condens. Matter **26**, 123202 (2014).

[8] B. Lenk, H. Ulrichs, F. Garbs, and M. Münzenberg, Phys. Rep. **507**, 4 (2011).

[9] R. Zivieri, Solid State Phys. **63**, 151 (2012).

[10] V. V. Kruglyak *et al.*, in *Magnonic Metamaterials*, edited by X.-Y. Jiang (InTech, London, 2012).

[11] C.-M. Hu, Physics in Canada **72**, 76 (2016).

[12] Ö. O. Soykal and M. E. Flatté, Phys. Rev. Lett. **104**, 077202 (2010).

[13] Ö. O. Soykal and M. E. Flatté, Phys. Rev. B **82**, 104413 (2010).

[14] L. Bai, M. Harder, Y. P. Chen, X. Fan, J. Q. Xiao, and C.-M. Hu, Phys. Rev. Lett. **114**, 227201 (2015).

[15] S. Kaur, B. M. Yao, J. W. Rao, Y. S. Gui, and C.-M. Hu, Appl. Phys. Lett. **109**, 032404 (2016).

[16] B. Z. Rameshti, Y. Cao, and G. E. W. Bauer, Phys. Rev. B **91**, 214430 (2015).

[17] Y. Tabuchi, S. Ishino, T. Ishikawa, R. Yamazaki, K. Usami, and Y. Nakamura, Phys. Rev. Lett. **113**, 083603 (2014).

[18] X. Zhang, C.-L. Zou, L. Jiang, and H. X. Tang, Phys. Rev. Lett. **113**, 156401 (2014).

[19] X. Zhang, C.-L. Zou, L. Jiang, and H. X. Tang, Science Advances **2**, 1501286 (2016).

[20] M. Goryachev, W. G. Farr, D. L. Creedon, Y. Fan, M. Kostylev, and M. E. Tobar, Phys. Rev. Applied **2**, 054002 (2014).

[21] J. Bourhill, N. Kostylev, M. Goryachev, D. L. Creedon, and M. E. Tobar, Phys. Rev. B **93**, 144420 (2016).

[22] J. Krupka, B. Salski, P. Kopyt, and W. Gwarek, Sci. Rep. **6**, 34739 (2016).

[23] J. Krupka, P. Aleshkevych, B. Salski, P. Kopyt, and A. Pacewicz, Sci. Rep. **7**, 5750 (2017).

[24] R. G. E. Morris, A. F. van Loo, S. Kosen, and A. D. Karenowska, Sci. Rep. **7**, 11511 (2017).

[25] H. L. Hu and F. R. Morgenthaler, Appl. Phys. Lett. **18**, 307 (1971).

[26] P. Fleury, S. Porto, L. Cheesman, and H. Guggenheim, Phys. Rev. Lett. **17**, 84 (1966).

[27] J. R. Sandercock and W. Wettling, Solid State Commun. **13**, 1729 (1973).

[28] P. Grunberg and F. Metawe, Phys. Rev. Lett. **39**, 1561 (1977).

[29] R. E. Camley and D. L. Mills, Phys. Rev. B **18**, 4821 (1978).

[30] M. Grimsditch, A. Malozemoff, and A. Brunsch, Phys. Rev. Lett. **43**, 711 (1979).

[31] M. G. Cottam, J. Phys. C **16**, 1573 (1983).

[32] B. Hillebrands, P. Baumgart, and G. Güntherodt, Phys. Rev. B **36**, 2450(R) (1987).

[33] J. Cochran and J. Dutcher, J. Appl. Phys. **63**, 3814 (1988).

[34] J. Jorzick, S. O. Demokritov, C. Mathieu, B. Hillebrands, B. Bartenlian, C. Chappert, F. Rousseaux, and A. N. Slavin, Phys. Rev. B **60**, 15194 (1999).

[35] S. O. Demokritov, B. Hillebrands, and A. N. Slavin, Phys. Rep. **348**, 441 (2001).

[36] E. Meloche, M. G. Cottam, V. P. Gnezdilov, and D. J. Lockwood, Phys. Rev. B **81**, 024426 (2010).

[37] T. Sebastian, K. Schultheiss, B. Obry, B. Hillebrands, and H. Schultheiss, Front. Phys. **3**, 35 (2015).

[38] S. Demokritov and E. Tsymbal, J. Phys.: Condens. Matter **6**, 7145 (1994).

[39] G. Carlotti and G. Gubbiotti, Nuovo Cimento **22**, 1 (1999).

[40] A. D. Fisher, Circuits Syst. Signal Process. **4**, 265 (1985).

[41] Yu. K. Fetisov and A. A. Klimov, J. Opt. Soc. Am. B **22**, 274 (2005).

[42] D. D. Stancil and A. Prabhakar, *Spin Waves-Theory and Applications* (Springer, Boston, 2009).

[43] J. A. Haigh, S. Langenfeld, N. J. Lambert, J. J. Baumberg, A. J. Ramsay, A. Nunnenkamp, and A. J. Ferguson, Phys. Rev. A **92**, 063845 (2015).

[44] A. Osada, R. Hisatomi, A. Noguchi, Y. Tabuchi, R. Yamazaki, K. Usami, M. Sadgrove, R. Yalla, M. Nomura, and Y. Nakamura, Phys. Rev. Lett. **116**, 223601 (2016).

[45] X. Zhang, N. Zhu, C.-L. Zou, and H. X. Tang, Phys. Rev. Lett. **117**, 123605 (2016).

[46] J. A. Haigh, A. Nunnenkamp, A. J. Ramsay, and A. J. Ferguson, Phys. Rev. Lett. **117**, 133602 (2016).

[47] Yu. S. Dadoenkova, N. N. Dadoenkova, I. L. Lyubchanskii, J. W. Klos, and M. Krawczyk, J. Appl. Phys. **120**, 073903 (2016).

[48] R. Hisatomi, A. Osada, Y. Tabuchi, T. Ishikawa, A. Noguchi, R. Yamazaki, K. Usami, and Y. Nakamura, Phys. Rev. B **93**, 174427 (2016).

[49] T. Y. Liu, X. F. Zhang, H. X. Tang, and M. E. Flatté, Phys. Rev. B **94**, 060405(R) (2016).

[50] S. V. Kusminskiy, H. X. Tang, and F. Marquardt, Phys. Rev. A **94**, 033821 (2016).

[51] P. A. Pantazopoulos, N. Stefanou, E. Almpanis, and N. Papanikolaou, Phys. Rev. B **96**, 104425 (2017).

[52] S. Sharma, Y. M. Blanter, and G. E. W. Bauer, Phys. Rev. B **96**, 094412 (2017).

[53] A. Osada, A. Gloppe, R. Hisatomi, A. Noguchi, R. Yamazaki, M. Nomura, Y. Nakamura, and K. Usami, Phys. Rev. Lett. **120**, 133602 (2018).

[54] A. Osada, A. Gloppe, Y. Nakamura, and K. Usami, arXiv:1711.09321.

[55] G. Gantzounis and N. Stefanou, Phys. Rev. B **73**, 035115 (2006).

[56] P. S. Pershan, J. Appl. Phys. **38**, 1482 (1967).

[57] L. D. Landau and E. M. Lifshitz, *Electrodynamics of Continuous Media* (Pergamon, Oxford, 1960).

[58] A. Christofi and N. Stefanou, Int. J. Mod. Phys. B **28**, 1441012 (2014).

[59] A. Christofi, N. Stefanou, and N. Papanikolaou, Phys. Rev. B **89**, 214410 (2014).

[60] P. Varytis, N. Stefanou, A. Christofi, and N. Papanikolaou, J. Opt. Soc. Am. B **32**, 1063 (2015).

[61] P. Varytis, P. A. Pantazopoulos, and N. Stefanou, Phys. Rev. B **93**, 214423 (2016).
[62] T. Inui, Y. Tanabe, and Y. Onodera, *Group Theory and Its Applications in Physics* (Springer-Verlag, Berlin, 1990).
[63] G. Gantzounis, J. Phys. Chem. C **113**, 21560 (2009).
[64] M. I. Mishchenko, L. D. Travis, and A. A. Lacis, *Scattering, Absorption, and Emission of Light by Small Particles* (Cambridge University Press, Cambridge, England, 2002).
[65] Z. Lin and S. T. Chui, Phys. Rev. E **69**, 056614 (2004).
[66] J. L.-W. Li, W.-L. Ong, and K. H. R. Zheng, Phys. Rev. E **85**, 036601 (2012).
[67] G. Gantzounis, N. Papanikolaou, and N. Stefanou, Phys. Rev. B **84**, 104303 (2011).
[68] M. Jafelicci, Jr. and R. H. M. Godoi, J. Magn. Magn. Mater. **226**, 1421 (2001).
[69] Y. J. Wu, H. P. Fu, R. Y. Hong, Y. Zheng, and D. G. Wei, J. Alloys Compd. **470**, 497 (2009).
[70] R. Y. Hong, Y. J. Wu, B. Feng, G. Q. Di, H. Z. Li, B. Xud, Y. Zheng, and D. G. Wei, J. Magn. Magn. Mater **321**, 1106 (2009).
[71] A. Zvezdin and V. Kotov, *Modern Magnetooptics and Magnetooptical Materials* (IOP Publishing, Bristol, England, 1997).
[72] V. E. Demidov, U. H. Hansen, and S. O. Demokritov, Phys. Rev. Lett. **98**, 157203 (2007).
[73] E. R. J. Edwards, M. Buchmeier, V. E. Demidov, and S. O. Demokritov, J. Appl. Phys. **113**, 103901 (2013).
[74] E. Almpanis, N. Papanikolaou, and N. Stefanou, Opt. Express **22**, 31595 (2014).